Effect of Anthropogenic Aerosol Addition on Phytoplankton Growth in Coastal Waters: Role of Enhanced Phosphorus Bioavailability

Qin Wang[1,2], Chao Zhang[1,2], Haoyu Jin[1,2], Ying Chen[3], Xiaohong Yao[1,2] and Huiwang Gao[1,2]*

[1] Key Laboratory of Marine Environment and Ecology, Frontiers Science Center for Deep Ocean Multispheres and Earth System, Ocean University of China, Ministry of Education of China, Qingdao, China, [2] Laboratory for Marine Ecology and Environmental Sciences, Pilot National Laboratory for Marine Science and Technology, Qingdao, China, [3] Shanghai Key Laboratory of Atmospheric Particle Pollution Prevention, Department of Environmental Science and Engineering, Fudan University, Ministry of Education of China, Shanghai, China

Atmospheric deposition can supply nutrients to induce varying responses of phytoplankton of different sizes in the upper ocean. Here, we collected surface and subsurface chlorophyll a maximum (SCM) seawaters from the Yellow Sea and East China Sea to conduct a series of onboard incubation experiments, aiming to explore the impact of anthropogenic aerosol (AR, sampled in Qingdao, a coastal city in Northern China) addition on phytoplankton growth using schemes with (unfiltered seawater, UFS) and without (filtered seawater, FS) microsized (20–200 μm) cells. We found that AR addition stimulated phytoplankton growth obviously, as indicated by chlorophyll a (Chl a) in surface incubations, and had stimulatory or no effects in SCM incubations, which was related to nutrient statuses in seawater. The high ratio of nitrogen (N) to phosphorus (P) in the AR treatments demonstrated that P became the primary limiting nutrient. The alkaline phosphatase activity (APA), which can reflect the rate at which dissolved organic P (DOP) is converted into dissolved inorganic P, was 1.3–75.5 times higher in the AR treatments than in the control, suggesting that AR addition increased P bioavailability in the incubated seawater. Dinoflagellates with the capacity to utilize DOP showed the dominant growth in the AR treatments, corresponding to the shift in phytoplankton size structure toward larger cells. Surprisingly, we found that nanosized (2–20 μm) and picosized (0.2–2 μm) Chl a concentrations in UFS were generally higher than those in FS. The APA in UFS was at least 1.6 times higher than in FS and was proportional to the contribution of microsized cells to the total Chl a, suggesting that microsized cells play an important role in the increase in APA, which contributes to the growth of nanosized and picosized phytoplankton. Current work provides new insight into the increase of P bioavailability induced by atmospheric deposition and resultant ecological effect in coastal waters.

Keywords: atmospheric deposition, nutrients, phytoplankton, size structure, China coastal waters, alkaline phosphatase

INTRODUCTION

Atmospheric deposition can supply a considerable amount of nutrients, including macronutrients such as nitrogen (N) and phosphorus (P), and micronutrients such as iron (Fe) and zinc (Zn), to the ocean (Jickells et al., 2005; Hooper et al., 2019), and affect the phytoplankton size structure and community composition (Okin et al., 2011; Marañón et al., 2015; Zhang et al., 2019). The deposition of a large amount of N promoted the growth of diatoms and inhibited the growth of diazotrophs in the Bay of Bengal and the Arabian Sea (Krishnamurthy et al., 2007). Dust additions increased the N:P ratios in the seawater and induced the dominant growth of nanosized (2–20 µm) phytoplankton in the East China Sea (ECS) (Zhang et al., 2019). The shift in phytoplankton size structure is always accompanied by the competition for nutrients among phytoplankton of different sizes (Stolte and Riegman, 1996; Hutchins et al., 1999). Large phytoplankton (≥2 µm in cell size) have a greater capacity for biomass accumulation and anti-predator defense (Agusti and Kalff, 1989; Finkel, 2007), leading to an advantageous growth in eutrophic seawater. With minimal diffusion boundary layer thickness and a larger specific surface area (Pasciak and Gavis, 1974; Finkel, 2007; Marañón, 2015; Wei et al., 2019), picosized (0.2–2 µm in cell size) phytoplankton have a competitive advantage in oligotrophic seawater (Chisholm, 1992; Finkel, 2007). However, this consensus is roughly defined, and the nutrient competition mechanism between phytoplankton of different sizes is rather complicated in realistic conditions, where the trophic status is not ideally eutrophic or oligotrophic (Chisholm, 1992; Finkel, 2007). For example, in contrast to diatoms, dinoflagellates have a growth advantage in high-nitrate and low-phosphate seawaters due to their acclimatization to high ratios of N:P (Moore et al., 2013; Zhang et al., 2019), even if there is an overlap in the size structure of diatoms and dinoflagellates. In high nutrient low chlorophyll (HNLC) and coastal seawaters, dust additions can induce the rapid growth of different kinds of diatoms covering nanosized and microsized cells (Boyd et al., 2007; Zhang et al., 2018). Our quantitative knowledge of the relationship between nutrient uptake and the growth of different sized phytoplankton is still inadequate.

The impact of atmospheric deposition on primary productivity is generally associated with the substantial supply of N and/or Fe nutrients, whereas few studies focus on P due to its negligible supply relative to N and Fe (Okin et al., 2011; Kim et al., 2014; Wu et al., 2018). Although some studies pointed out that atmospheric deposition can promote the utilization of DOP to relieve P limitation by providing cofactors such as Fe and Zn in open oceans primarily characterized by oligotrophy (Mahaffey et al., 2014; Browning et al., 2017), there are few studies reported in coastal waters characterized by mesotrophy and even eutrophy. In the context of the overwhelming input of N relative to P through various ways such as riverine input and atmospheric deposition, the phenomenon of P limitation becomes increasingly prevailing in coastal waters (Zheng and Zhai, 2021). The impact of atmospheric deposition on marine phytoplankton is not only confined to the traditional relationship between supply (e.g., N and Fe supply) and demand (e.g., N

and Fe limitation), but also considering the acclimatization mechanism to copy with the potential P deficiency. A few studies have deduced that atmospheric deposition might enhance the utilization of DOP in P-deficient environments by calculating the P budget in the system and setting up model parameters (Chu et al., 2018; Zhang et al., 2018). However, there is still a lack of direct evidence to verify this hypothesis in coastal waters, and the resultant ecological effect is still poorly understood.

The Yellow Sea (YS) and ECS adjacent to the East Asian continent are marginal seas of the northwestern Pacific Ocean and are obviously influenced by anthropogenic air pollutants from the surrounding continent (Wang et al., 2000; Zhang and Gao, 2007). A series of studies reported that anthropogenic aerosols can transport a long distance to reach coastal seas and even open oceans (Fu et al., 2015; Kang et al., 2017; Xiao et al., 2018). The source apportionment results also showed that particles collected in the YS were full of secondary, biomass burning, and soot-like particles, indicating that marine aerosols are strongly affected by anthropogenic activities (Du et al., 2012; Fu et al., 2015; An et al., 2019). The N:P ratio in anthropogenic aerosol (AR) is generally much higher than the phytoplankton stoichiometry (i.e., Redfield ratio: N:P = 16:1). In the Jiaozhou Bay of the YS, the N:P ratio of atmospheric dry deposition is higher than 100 and even exceeds 1,000 in some specific conditions (Xing et al., 2017; Wu et al., 2018). It has been reported that anthropogenic N deposition has the potential to change nutrient structure in the seawater (Kim et al., 2014). Atmospheric N deposition is regarded as an important factor that induces phytoplankton blooms (Tan and Shi, 2012; Tan and Wang, 2014). On the other hand, under the impact of vertical water mixing, the nutrients in atmospheric deposition can be transferred to the subsurface layers. Model studies have shown that the supplementation of N in surface waters to the lower layer is an important reason for the formation of subsurface chlorophyll *a* maximum (SCM) (Hodges and Rudnick, 2004; Gong et al., 2017). In contrast to the surface layer, few studies focused on the impact of atmospheric deposition on phytoplankton in the SCM layer.

In this study, we carried out three onboard incubation experiments enriched with AR using surface and SCM seawaters in the YS and ECS. The unfiltered and filtered (through 20-µm membrane) seawaters were used to illustrate the effects of microsized (20–200 µm) phytoplankton on the growth and nutrient uptake of nanosized (2–20 µm) and picosized ones. Based on this, our study intended to (1) reveal the difference in phytoplankton response to AR addition in surface and SCM seawaters; (2) identify the main factor of AR addition that affects the growth and community structure succession of phytoplankton; and (3) explore the interaction between different sized phytoplankton under the effects of AR addition.

MATERIALS AND METHODS

Incubation Experiments

The AR samples used for incubation experiments were collected with a cellulose acetate filter membrane (Whatman 41) on the Laoshan campus of Ocean University of China (36°9′39″N,

120°29'29"E) on 30 June 2019. During the sampling period, the AQI was 57–83 μg m^{-3}, indicating that the air quality is moderate. The detailed air quality conditions are shown in **Table 1**.

In the summer of 2019, three onboard microcosm experiments were conducted during the cruise of R/V Beidou in the YS and the northern part of the ECS (**Figure 1A**). The initial seawater at U1, U2 and U3 was collected from surface layers ($\sim$3–5 m below the water surface) and SCM layers (captured by the CTD profile data) using Niskin bottles with Sea Bird CTD-General Oceanic Rosette assembly (**Table 2**). The site name is abbreviated as Ui$_{Sur}$ and Ui$_{SCM}$, respectively, and i refers to the site number, i.e., 1/2/3.

Based on the content of N in AR aerosols, three treatments were conducted in triplicate for the incubation experiments: (1) control, no AR addition; (2) low AR addition, the added amount of AR was expressed in the unit of N (i.e., 1 μmol N L^{-1}) at U2, indicating that the added amount of AR contains 1 μmol N L^{-1}; (3) high AR addition, 1.7 μmol N L^{-1} at U3, and 2 μmol N L^{-1} at U1. AR sample was first ultrasonically extracted in deionized water at 0°C for 1 h, and the leaching solution including particles was added to the incubation bottles directly (Guo et al., 2013). Apart from inorganic nutrients, the aerosol additions could stimulate mixotrophic dinoflagellates by promoting the utilization of organic matter (Granéli et al., 1999; Heisler et al., 2008; Lin et al., 2012). With N addition of 1 μmol L^{-1}, 1.7 μmol L^{-1}, and 2 μmol L^{-1} by AR particles, the P concentrations added by AR particles were only 17.98, 30.56, and 35.95 nmol L^{-1}. The added amount of AR was determined according to the deposition flux of N (574.0–970.0 mg m^{-2} event^{-1}) divided by an averaged mixed layer of 30 m (Shi et al., 2012; Sin et al., 2013). Nutrient enrichment experiments were set up to illustrate nutrient limitation in original seawaters and interpret phytoplankton response to AR additions (**Supplementary Table 1**).

The sampled seawater was passed through 200-μm sieves, mixed well in a clean 120-L high-density polyethylene barrel, and then dispensed into clean (acid-washed) 20-L polycarbonate incubation bottles. These incubation bottles were placed into three microcosm devices filled with continually updated surface seawater to keep the incubation system temperature relatively stable (Zhang et al., 2019). To explore the impact of microsized cells on the phytoplankton community, seawater from incubation bottles of each treatment was filtered through 20-μm sieves when the contribution of microsized Chl a to total Chl a in the control exceeded 20%, and then, the filtered seawater (hereafter FS) was transferred uniformly into three 2-L bottles to continue the cultivation. The incubations unfiltered with 20-μm sieves were defined as the unfiltered seawater (hereafter UFS, **Figure 1B**). Bottles were shaded to have approximately 40% light attenuation, matching light levels at depths on 3–5 m as previously used (Zhang et al., 2019, 2020). All experiments ran for 5–6 days.

Measurements of Chlorophyll a, Nutrients, and the Phytoplankton Community Structure

Chlorophyll a

Approximately 150 ml of seawater from incubated bottles was sampled at $\sim$07:00 a.m. every day during the incubations. The sampled seawater was subsequently filtered through 20-, 2-, and 0.2-μm filters, to obtain microsized, nanosized, and picosized cells. After 20–24 h of extraction by 90% acetone in darkness at –20°C, the pigments collected by different filters were measured using a Trilogy fluorometer (Turner Designs). The total Chl a concentration was obtained by summing three size-fractionated Chl a concentrations.

Nutrients

An ultrasonic method was used to leach nutrients in AR samples. Briefly, AR samples were ultrasonically extracted in deionized water at 0°C for 1 h. The leaching solution was then filtered through a 0.45-μm polyethersulfone syringe filter (Shi et al., 2010). The filtrates were used for the determination of soluble nutrients from aerosols, including NO_3^-, NO_2^-, NH_4^+, $Si(OH)_4$, and PO_4^{3-}. In addition, $\sim$200 ml of incubated seawater (sampled every day) was filtered through acid-washed cellulose acetate membranes into 125-ml acid-washed high-density polyethylene bottles (prerinsed with the filtrates three times). The water samples were frozen at -20°C immediately prior to the determination of $NO_3^- + NO_2^-$, PO_4^{3-}, and $Si(OH)_4$ in the university laboratory. All nutrient samples were measured with a QuAAtro continuous-flow analyzer (SEAL Analytical). The detection limits for NH_4^+, NO_3^-, NO_2^-, PO_4^{3-}, and $Si(OH)_4$ were 0.04, 0.02, 0.005, 0.01, and 0.03 μmol L^{-1}, respectively. For convenience, $NO_3^- + NO_2^-$ is abbreviated to N + N.

TABLE 1 | Air quality conditions during the anthropogenic aerosol (AR) sampling period.

Parameter	Concentration
Humidity (%)	62–91
AQI (μg$\cdot$m^{-3})	57–83
PM$_{2.5}$ (μg$\cdot$m^{-3})	29–61
PM$_{10}$ (μg$\cdot$m^{-3})	63–94
NH$_4^+$ (μmol$\cdot$m^{-3})	0.17
NO$_3^-$ + NO$_2^-$ (μmol$\cdot$m^{-3})	0.43
PO$_4^{3-}$ (nmol$\cdot$m^{-3})	7.37
Fe (nmol$\cdot$m^{-3})	31.88
Zn (nmol$\cdot$m^{-3})	2.31
Al (nmol$\cdot$m^{-3})	72.24
Mn (nmol$\cdot$m^{-3})	0.98
Cu (nmol$\cdot$m^{-3})	0.19
Cd (nmol$\cdot$m^{-3})	0.01
Ni (nmol$\cdot$m^{-3})	0.13
Pb (nmol$\cdot$m^{-3})	0.13
Co (nmol$\cdot$m^{-3})	0.01

Humidity data during sampling were obtained from National Meteorological Information Center (NMIC, https://data.cma.cn/). AQI, PM$_{2.5}$, and PM$_{10}$, were obtained from China National Environmental Monitoring Center (CNEMC, http://www.cnemc.cn/). The soluble nutrients and total trace metal concentrations in aerosols were sampled and determined in the laboratory (Zhao et al., 2015).

The concentrations of total trace metals were analyzed by inductively coupled plasma mass spectrometry (ICP-MS) (Shi et al., 2012). The 8-cm^2 cellulose acetate filter was put into the Teflon high pressure vial, with 2 ml of 69% HNO_3 and 0.5 ml of 40% HF. After digestion at 180°C for 48 h, the solution was evaporated at 160°C, the residue was dissolved with 2% HNO_3 and diluted to 50 ml for determination.

Alkaline Phosphatase Activity

About 45 ml of seawater was sampled from the incubated bottles and mixed with 0.5 ml of fluorogenic substrate 4-methylumbelliferone phosphate (MUF-P) as the mixed substrate. After the addition of the mixed borax-sodium carbonate buffer solution (pH = ~11) and the mixed substrate to the sample tube, the fluorogenic substrate MUF-P hydrolyzed by

AP was converted into equimolar phosphate group and 4-methylumbelliferone (MUF). The fluorescence value of MUF was measured and recorded by a Trilogy fluorometer (Turner Designs) at 0, 0.5, and 1 h (Sebastián et al., 2004). The slope was calculated as the hydrolysis rate, which reflect the alkaline phosphatase activity (APA).
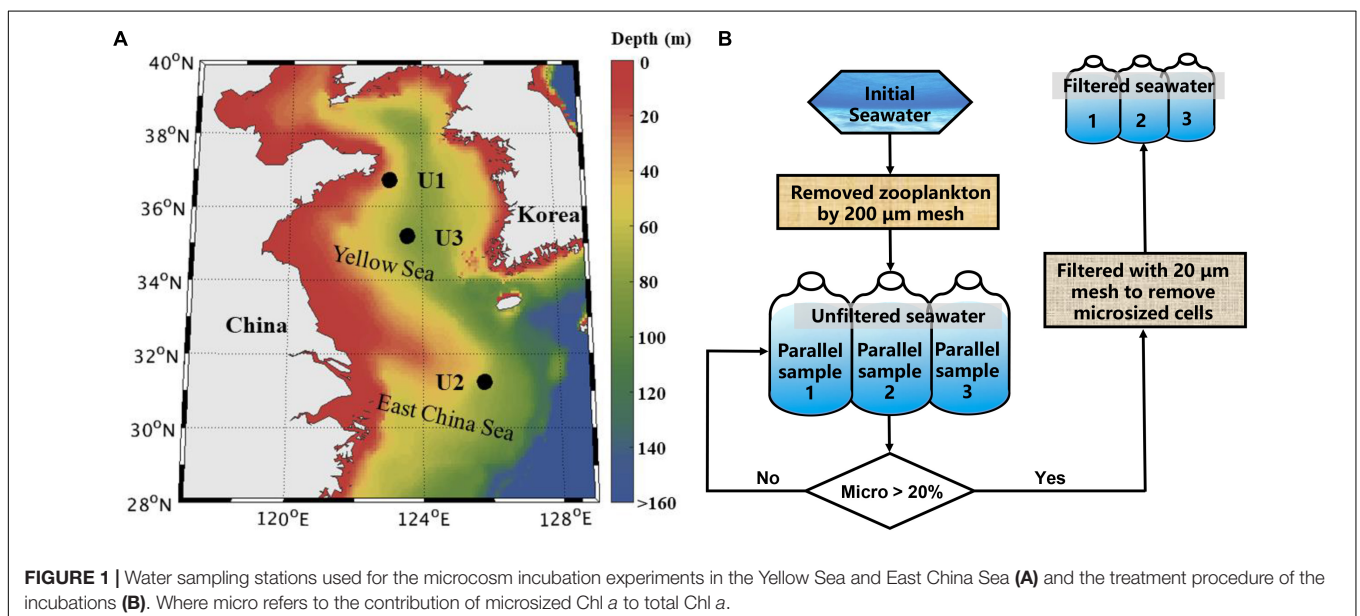
High-Throughput Sequencing

Approximately, 1 L of seawater from incubated bottles was filtered using 0.22-μm Whatman polycarbonate filters under gentle vacuum pressure (≤ 0.02 MPa). Filters were stored immediately in liquid nitrogen until DNA extraction and high-throughput sequencing (Shanghai Personal Biotechnology Co., Ltd., Shanghai, China). The V4 hypervariable region was selected as the target region of the 18S rDNA (Liu et al., 2021). The

TABLE 2 | Background conditions of seawater at the experimental sites.

Site	U1		U2		U3	
Incubation dates (2019)	Aug 16-21		Sep 3-8		Aug 22-28	
Water layer	Surface	SCM	Surface	SCM	Surface	SCM
Water depth (m)	3	19	3	34	3	29
Temperature (°C)	24.2	18.0	28.6	26.7	27.7	20.3
Salinity	31.5	31.8	31.4	32.8	30.2	32.6
$NO_3^- + NO_2^-$ (μmol·L^{-1})	0.19	1.70	0.08	2.59	0.10	0.11
PO_4^{3-} (μmol·L^{-1})	0.01	0.17	ND	0.11	0.01	0.01
$Si(OH)_4$ (μmol·L^{-1})	2.85	4.78	1.34	4.90	1.71	0.98
N:P (μmol:μmol)	15:1	10:1	20:1	24:1	12:1	11:1
APA (nmol·(L·h)$^{-1}$)	35.3	3.4	2.2	3.7	18.4	4.7
Chl a (μg·L^{-1})	0.38	1.19	0.55	0.95	0.62	0.58
Micro Chl a (%)	9	26	8	8	9	15
Nano Chl a (%)	18	22	27	30	36	38
Pico Chl a (%)	73	52	65	62	55	47
Dinophyceae (%)	60	95	85	89	92	96

ND, not detectable.

FIGURE 1 | Water sampling stations used for the microcosm incubation experiments in the Yellow Sea and East China Sea **(A)** and the treatment procedure of the incubations **(B)**. Where micro refers to the contribution of microsized Chl a to total Chl a.
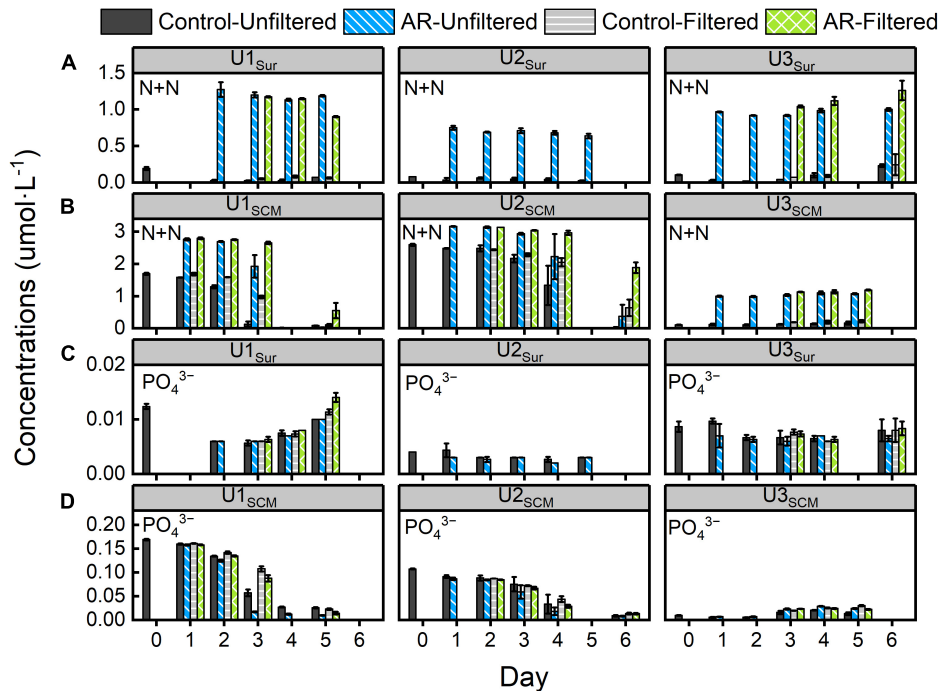
FIGURE 2 | Changes in panels **(A,B)** N + N and **(C,D)** PO_4^{3-} concentrations in the control and anthropogenic aerosol (AR) treatments incubated with surface and subsurface chlorophyll *a* maximum (SCM) seawaters. The error bar represents the standard deviation of three parallel samples.

primers for polymerase chain reaction (PCR) were forward primer 582F, 5'-CCAGCASCYGCGGTAATTCC-3' and reverse primer V4R, 5'-ACTTTCGTTCTTGATYRA-3' (Hernández-Ruiz et al., 2020). The Illumina NovaSeqPE250 platform was used for paired-end sequencing of community DNA fragments. First, we demultiplexed the raw sequence data and then invoked QIIME cutadapt trim-paired to cut the primers (Martin, 2011). Quality control of these sequences was performed using the DADA2 plugin with QIIME dada2 denoise-paired (Callahan et al., 2016). Then, we merged amplicon sequence variants (ASVs) and removed singleton ASVs. A pretrained naive Bayes classifier plugin was used to annotate the species for each ASV using QIIME2 software (2019.4) (Bokulich et al., 2018). The SILVA database (Release132)[1] (Quast et al., 2013) was used for species annotation. The microbiome bioinformatics of communities was analyzed using QIIME2 (2019.4). The accession number in NCBI Sequence Read Archive was PRJNA835313.

Data Analysis

We used one-way ANOVA to assess whether there was a significant difference in the Chl *a* concentration between the control and treatments (Andersen et al., 2020) and evaluated the nutrient limitation in surface seawater at the three sites. Statistical analysis was performed using IBM SPSS Statistics 20 (SPSS 20.0). CANOCO software (version 5.0) was used to analyze the relationships between environmental factors and phytoplankton. The detrended correspondence analysis (DCA)

used species-sample data showed that the first axis of gradient was less than 3. Therefore, redundancy analysis (RDA) was the better choice.
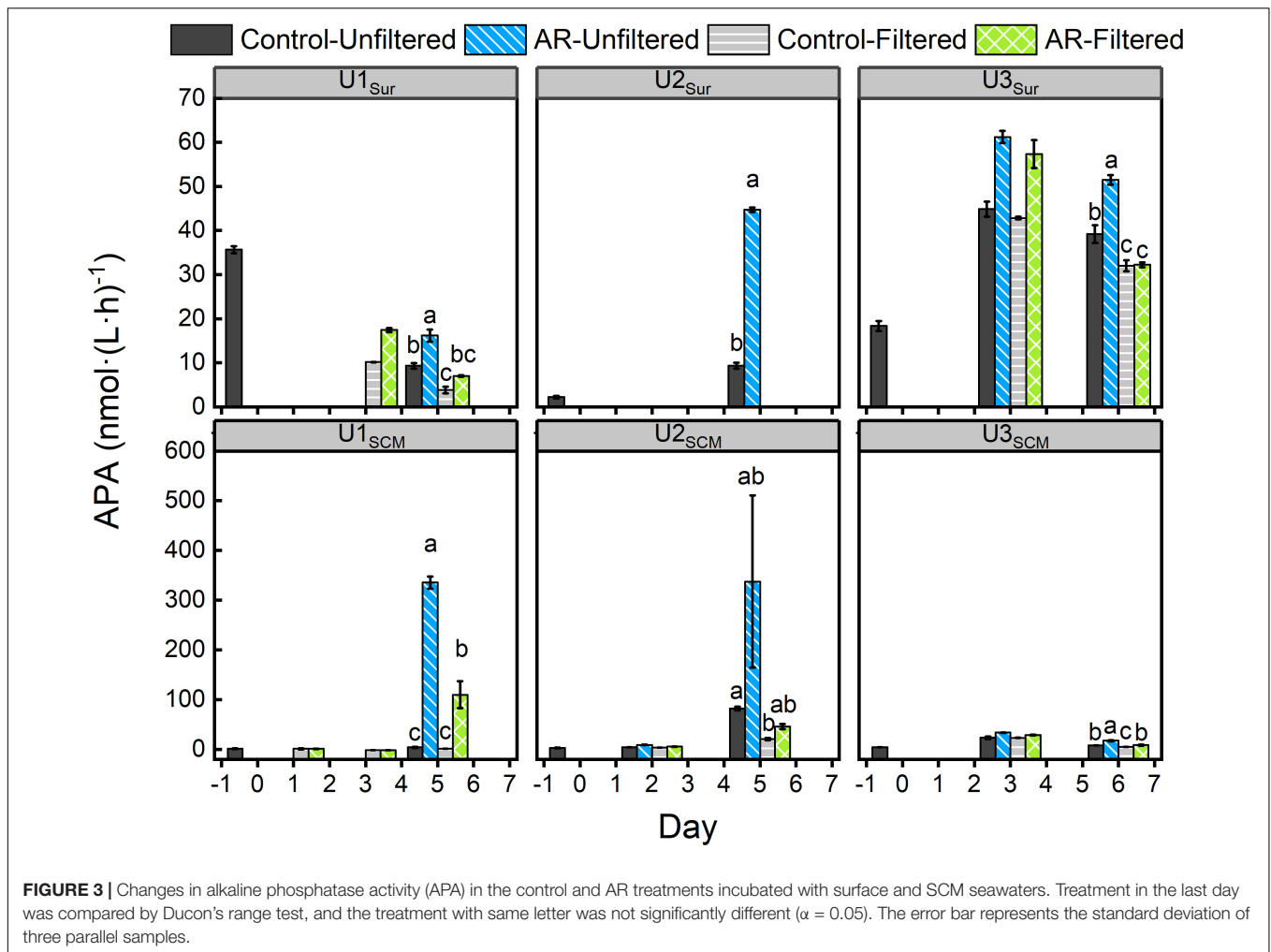
RESULTS

Overview of Original Seawater in Surface and Subsurface Chlorophyll *a* Maximum Layers

In general, trophic statuses in surface seawater at $U1_{Sur}$, $U2_{Sur}$, and $U3_{Sur}$ and in SCM seawater at $U3_{SCM}$ were lower than those in SCM seawater at $U1_{SCM}$ and $U2_{SCM}$. Phytoplankton at $U1\text{-}3_{Sur}$ were colimited by N and P based on the significant increase in Chl *a* after N + P addition relative to the control treatment (on days 4–6, $p < 0.05$, **Supplementary Figure 1**).

At $U1_{Sur}$, the concentrations of N + N, PO_4^{3-}, and $Si(OH)_4$ were 0.19, 0.01, and 2.85 µmol L^{-1}, respectively. APA was 35.3 nmol $(L\ h)^{-1}$ in the original seawater, consistent with the reported value of ∼35 nmol $(L\ h)^{-1}$ in this region (Wang et al., 2014). The total Chl *a* concentration was as low as 0.38 µg L^{-1}, of which picosized cells (73%) contributed to the most of the total Chl *a*, followed by nanosized cells (18%) and microsized cells (9%) (**Table 2**). Chloropicophyceae and Dinophyceae codominated the community, with a relative abundance of 33 and 60%, respectively.

At $U2_{Sur}$, $U3_{Sur}$ and $U3_{SCM}$, low concentrations of N + N and PO_4^{3-} were observed, i.e., 0.08-0.11 and ∼0.01 µmol L^{-1}, respectively. The APA was less than 18.4 nmol $(L\ h)^{-1}$, and the

FIGURE 3 | Changes in alkaline phosphatase activity (APA) in the control and AR treatments incubated with surface and SCM seawaters. Treatment in the last day was compared by Ducon's range test, and the treatment with same letter was not significantly different ($\alpha = 0.05$). The error bar represents the standard deviation of three parallel samples.

total Chl a concentration (0.55-0.62 μg L^{-1}) was more than 1.4 times higher than that at $U1_{Sur}$. Picosized Chl a contributed to the most of the total Chl a (47-65%), and the contribution of microsized Chl a was less than 15%. Dinophyceae dominated the communities with a relative abundance of $\geq$85% (**Table 2**).

Seawaters at $U1_{SCM}$ and $U2_{SCM}$ contained abundant nutrients, with 1.70-2.59 μmol L^{-1} of N + N, 0.11-0.17 μmol L^{-1} of PO$_4^{3-}$, and 4.78-4.90 μmol L^{-1} of Si(OH)$_4$. The APA at $U1_{SCM}$ and $U2_{SCM}$ [3.4-3.7 nmol (L h)$^{-1}$] was of the same orders of magnitude as those of $U2_{Sur}$ and $U3_{SCM}$. The total Chl a concentration ($\geq$0.95 μg L^{-1}) was more than 1.7 times higher than that of $U1_{Sur}$ and $U2_{Sur}$. Picosized phytoplankton (52-62%) were the primary contributors to the total Chl a. Dinophyceae dominated the communities with a relative abundance of $\geq$89% (**Table 2**).

Changes in Inorganic Nutrients

The N:P ratio after AR addition increased from 11:1-20:1 to 44:1-54:1 at all sites in the surface incubated seawater and at $U3_{SCM}$ in the SCM incubated seawater. Due to the sufficient nutrient stock in the original seawater at $U1_{SCM}$ and $U2_{SCM}$, the N supplied by AR addition only increased the N:P ratio from 10:1-24:1 to 16:1-28:1. Because of the low contents of PO$_4^{3-}$ and Si(OH)$_4$ in the AR, the changes in the concentrations of PO$_4^{3-}$ and Si(OH)$_4$ in AR-amended seawater were slight at all sites.

During the incubations at $U1$-3_{Sur} and $U3_{SCM}$, the concentrations of N + N did not change significantly in the control and AR treatments (**Figure 2**). In the AR treatments, the N + N concentrations remained relatively stable and were significantly higher than those in the control treatments. In contrast, the concentrations of PO$_4^{3-}$ were close to the detection limit in all treatments. The maximum consumption of Si(OH)$_4$ in the control and AR treatments was less than 13% at $U1$-3_{Sur} and $U3_{SCM}$. At $U1_{SCM}$ and $U2_{SCM}$, the concentrations of N + N and PO$_4^{3-}$ decreased gradually by more than 85% in the control and AR treatments relative to the original values. The concentrations of Si(OH)$_4$ decreased sharply in the control (>28%) and AR treatments (>69%) on days 3-5 at both sites (**Figure 2** and **Supplementary Figure 2**).

There were no obvious differences in the concentrations of N + N, PO$_4^{3-}$, and Si(OH)$_4$ between FS and UFS in the control and AR treatments at $U1$-3_{Sur} and $U3_{SCM}$. In the FS at $U1_{SCM}$ and $U2_{SCM}$, the consumption of N + N and Si(OH)$_4$ in AR treatments
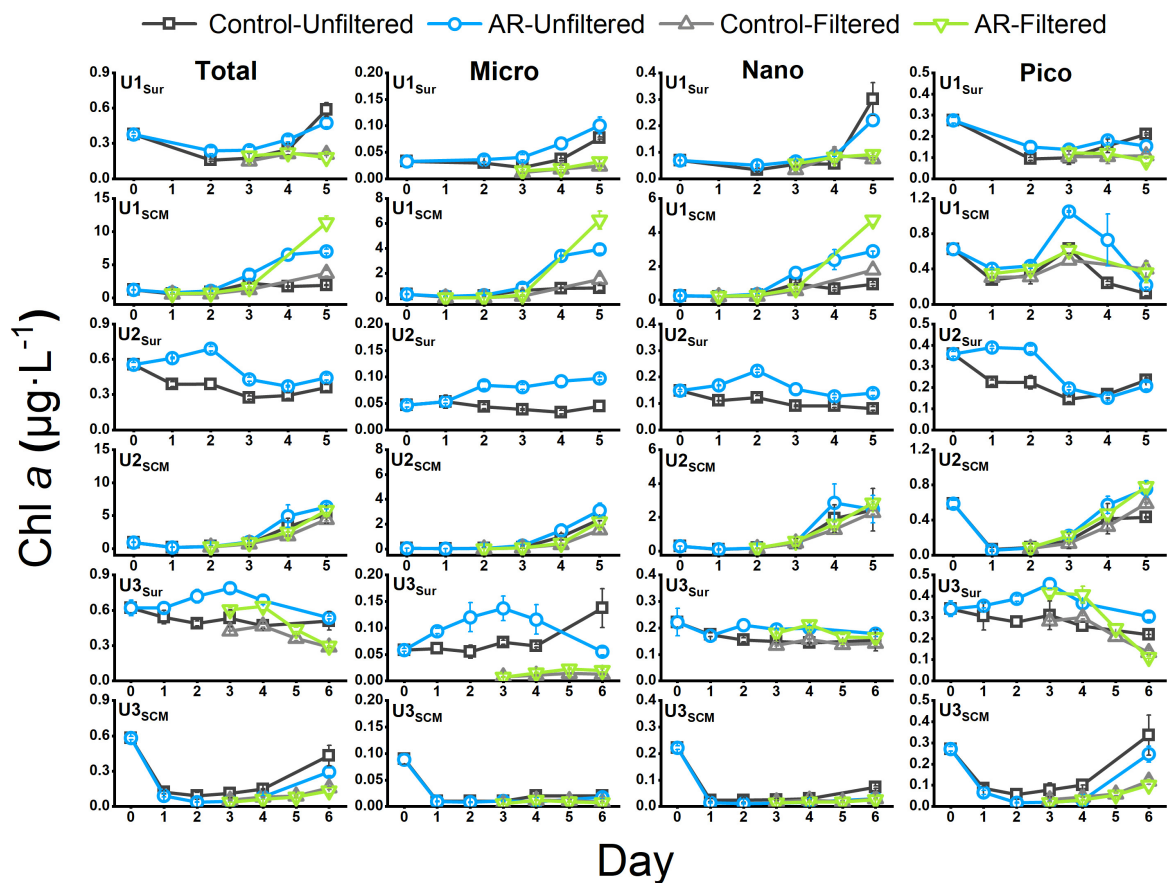
FIGURE 4 | The concentration of Chl *a* in the control and AR treatments incubated with surface and SCM seawaters. The error bar represents the standard deviation of three parallel samples.

was lower than that in the UFS at the end of the incubations ($p < 0.05$, **Figure 2** and **Supplementary Figure 2**).

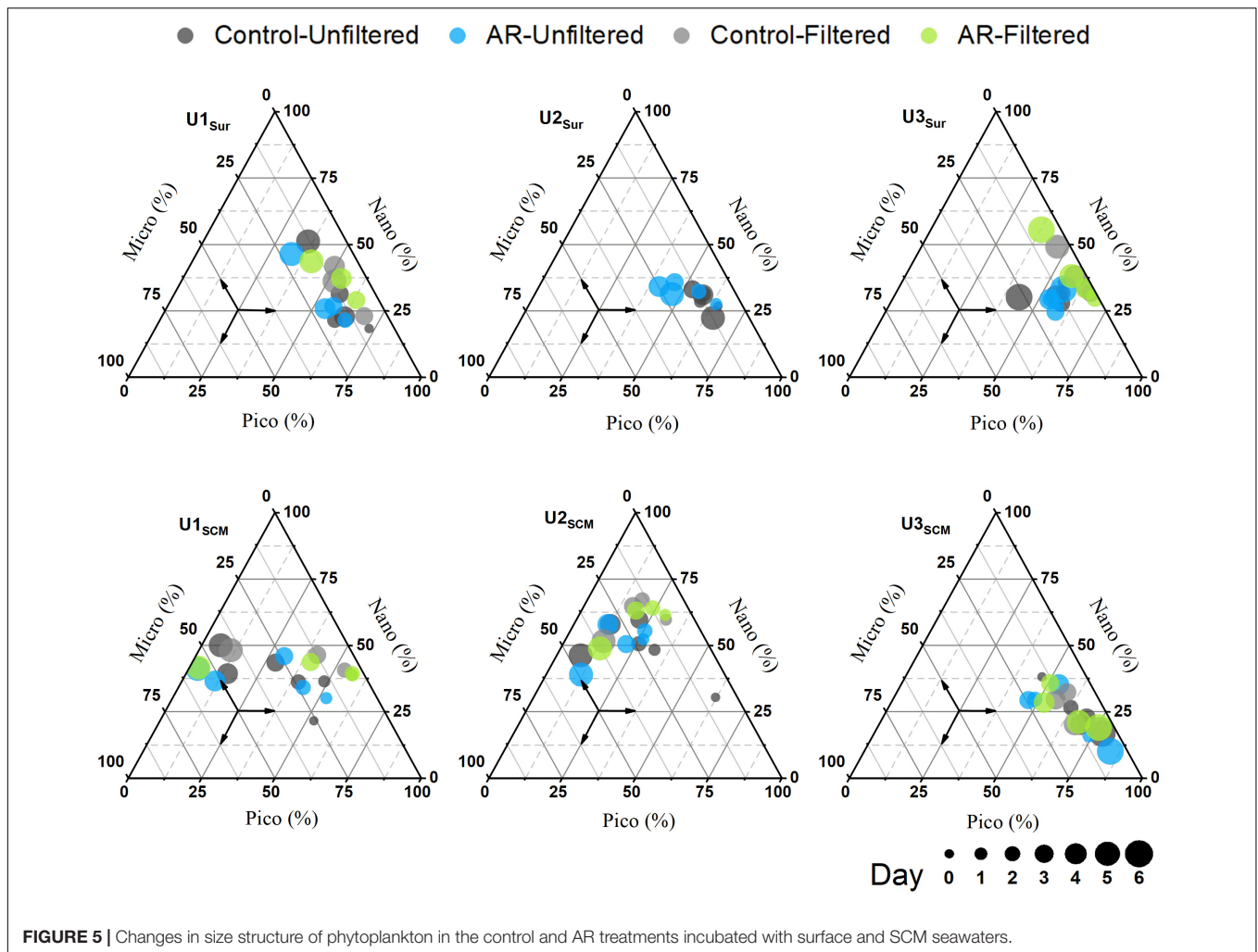## Changes in Alkaline Phosphatase Activity

In the UFS, the APA in the AR treatments was 1.3-75.5 times higher than that in the control at the end of the incubations ($p < 0.05$, **Figure 3**), and this phenomenon could be observed in both surface and SCM incubations. In contrast, there was almost no difference in APA between control and AR treatments on the last day of FS incubations at all sites except U1$_{SCM}$. For the AR treatments, the APA in the UFS at all sites was generally higher (1.6-7.3 times) than that in the FS (**Figure 3**).

Changes in Total and Size-Fractionated Chlorophyll *a*

At U1-3$_{Sur}$, the concentration of the total Chl *a* in the AR treatments was generally higher than that in the control. At U1$_{SCM}$, the total Chl *a* concentration in the AR treatments was more than 1.2 times higher than that in the control on days 2-5. At U2$_{SCM}$ and U3$_{SCM}$, there was no significant difference in Chl *a* between the control and AR treatments (**Figure 4**). The

responses of phytoplankton of different sizes varied with AR addition. At U1$_{Sur}$, the dominant size of phytoplankton changed from picosize to nanosize (46% contribution to total Chl *a*). A similar pattern in the size shift toward larger cells also occurred at U2$_{Sur}$ and U3$_{Sur}$, although picosized cells always dominated the contribution to total Chl *a* (**Figure 5**). At U1$_{SCM}$ and U2$_{SCM}$, the dominant contributor of phytoplankton in AR treatments was picosized cells on days 1-2 and shifted to microsized cells ($\geq$49% contribution to total Chl *a*) on day 5. At U3$_{SCM}$, the dominant contributor was always picosized phytoplankton during the incubations (**Figure 5**).

For AR treatments, the concentrations of nanosized and picosized Chl *a* in UFS were generally higher than those in FS at U1$_{Sur}$ and U3$_{Sur}$. Specifically, at U1$_{Sur}$, nanosized and picosized Chl *a* concentrations in the UFS enriched with AR were 2.4 and 1.8 times higher than those in the FS on day 5. At U3$_{Sur}$, the picosized Chl *a* concentration in UFS enriched with AR was 2.7 times higher than that in FS on day 6. Similar to the incubations with surface seawater, the picosized Chl *a* concentration enriched with AR in FS (0.10 µg L^{-1}) at U3$_{SCM}$ was lower than that in UFS (0.25 µg L^{-1}) on day 6. In contrast, at U1$_{SCM}$, nanosized and picosized Chl *a* concentrations in FS (4.72 and 0.36 µg L^{-1}) were higher than those in UFS (2.89 and 0.22 µg L^{-1}) on day 5. At

FIGURE 5 | Changes in size structure of phytoplankton in the control and AR treatments incubated with surface and SCM seawaters.

$U2_{SCM}$, there was no significant difference in the concentrations of size-fractionated Chl a between UFS and FS (**Figure 4**).

Changes in the Phytoplankton Community

The ASVs at all sites assigned to phytoplankton could be classified into 25 groups of eukaryotic microalgae at class level (level 3). The ASV richness of Dinophyceae (dinoflagellates) accounted for ≥60% of phytoplankton in the original seawater at each site. In terms of UFS, Dinophyceae dominated the phytoplankton community in the AR treatments at all sites (**Figure 6**). The dominant class changed from Dinophyceae to Chloropicophyceae (71%) in the control on day 5 of the incubations (corresponding to the maximum Chl a concentration) at $U1_{Sur}$. *Chloropicon* spp. was the main component of Chloropicophyceae (**Supplementary Figure 3**). With AR addition, the relative abundance of Dinophyceae increased to 46% being the dominant phytoplankton (**Figure 6**). The succession of phytoplankton communities at $U3_{SCM}$ was similar to that at $U1_{Sur}$. Dinophyceae maintained the dominant
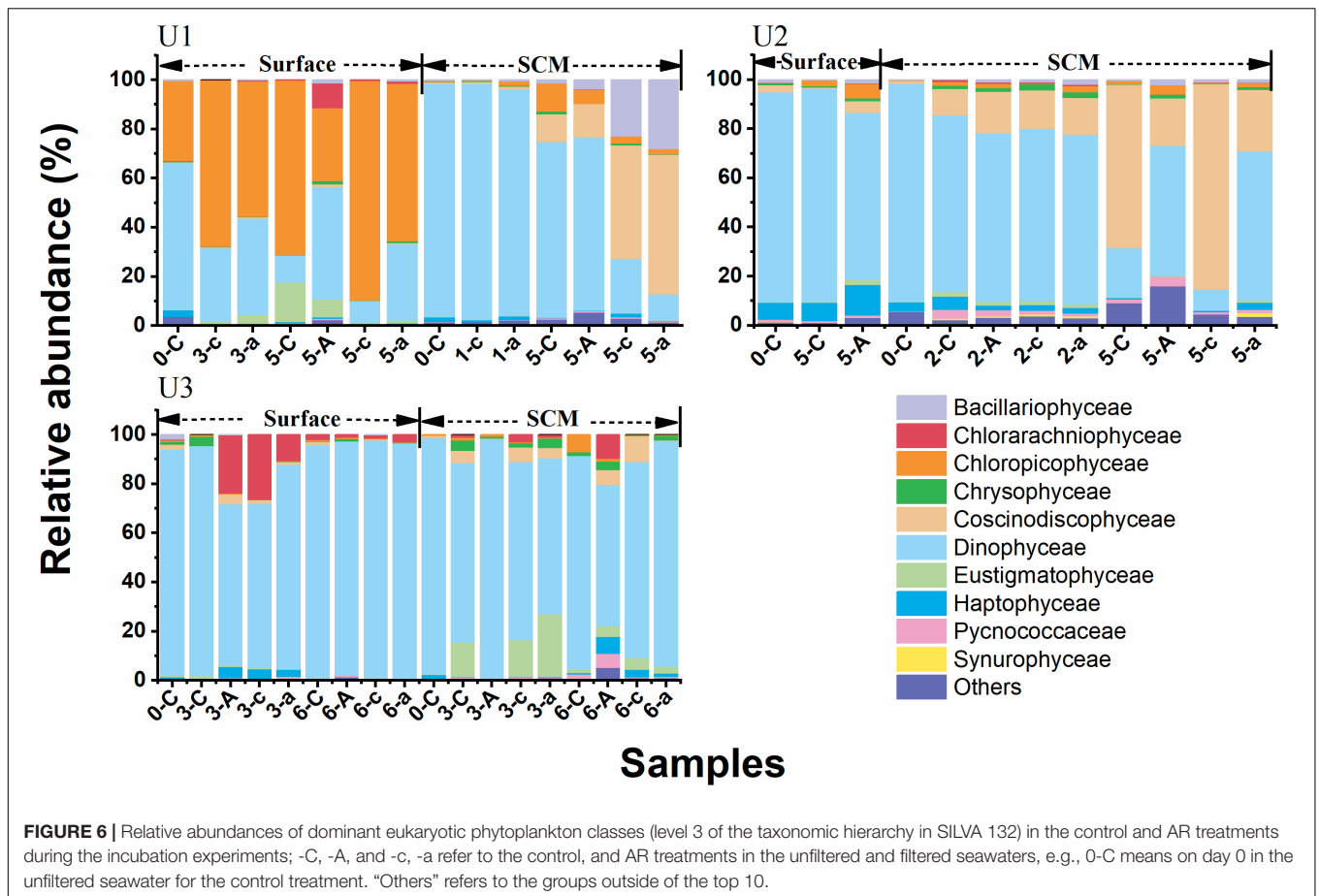
status in the control and AR treatments at the rest of the incubation sites (**Figure 6**).

DISCUSSION

Based on the distinct nutrient concentrations (N, P, and Si) in the original seawaters, the sites used for incubations were classified into two types: $U1-3_{Sur}$ and $U3_{SCM}$ with lower trophic status, where the concentrations of N + N, PO_4^{3-}, and $Si(OH)_4$ did not exceed 0.50, 0.02, or 3.00 μmol L^{-1}, respectively; $U1_{SCM}$ and $U2_{SCM}$ with higher trophic status, where the concentrations of N + N, PO_4^{3-}, and $Si(OH)_4$ exceeded 1.50, 0.10, and 4.50 μmol L^{-1}, respectively.

Distinct Responses of Phytoplankton to Anthropogenic Aerosol Additions in Surface and Subsurface Chlorophyll a Maximum Seawaters

Aerosol additions generally stimulated phytoplankton growth and shifted the phytoplankton size structure toward larger cells
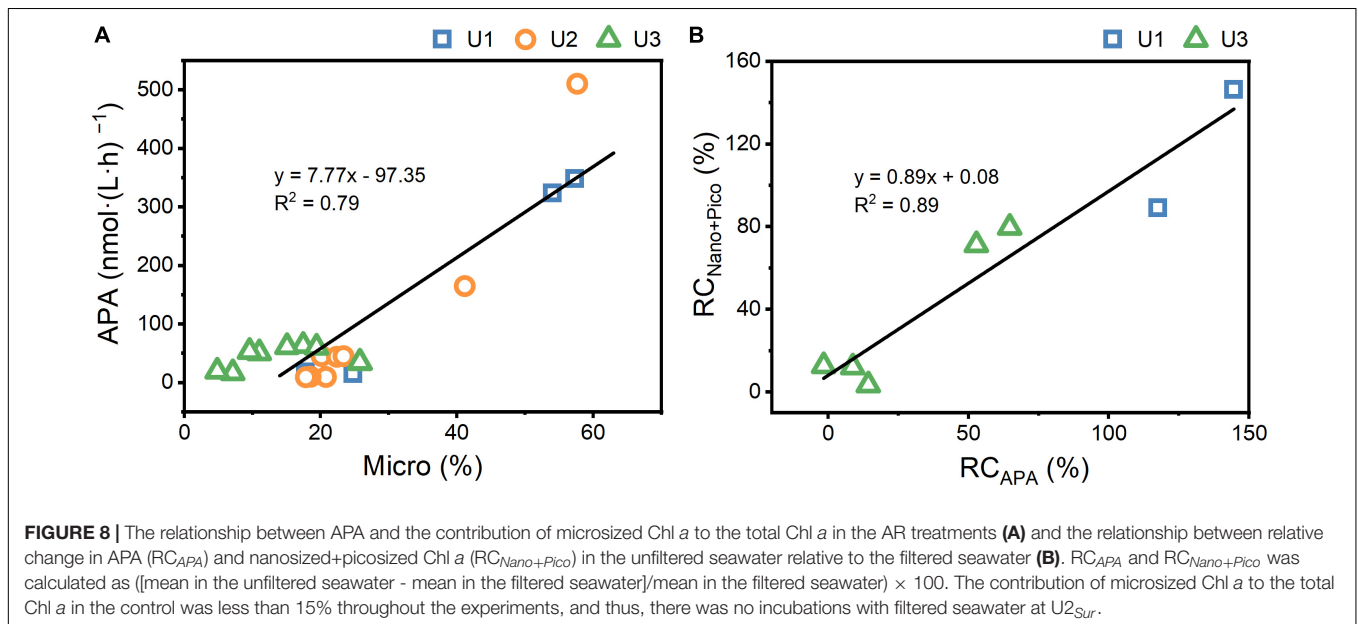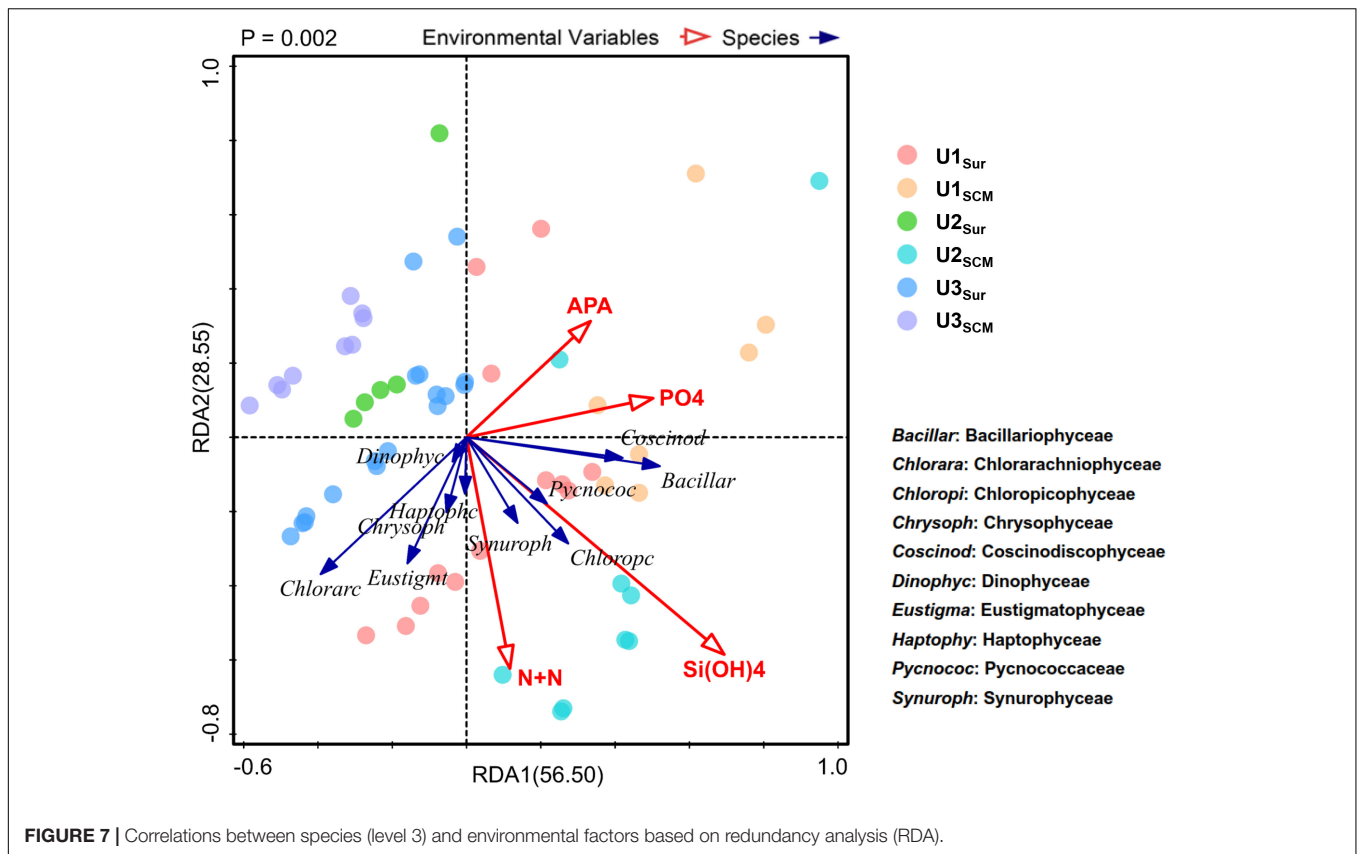
FIGURE 6 | Relative abundances of dominant eukaryotic phytoplankton classes (level 3 of the taxonomic hierarchy in SILVA 132) in the control and AR treatments during the incubation experiments; -C, -A, and -c, -a refer to the control, and AR treatments in the unfiltered and filtered seawaters, e.g., 0-C means on day 0 in the unfiltered seawater for the control treatment. "Others" refers to the groups outside of the top 10.

in surface incubated seawaters (**Figure 5**). This is justified because of the established supplementary relationship between nutrients (primarily N) supplied by AR and phytoplankton requirements. Such fertilization effect has also been widely reported in the previous studies (Cottingham, 1999; Liu et al., 2013; Zhang et al., 2019). In contrast, AR additions had a limited effect on phytoplankton size structure at U3$_{SCM}$, although its trophic status was similar to those in surface seawaters (**Figure 5**). This is ascribed to the photo-acclimation of phytoplankton under the condition of low irradiance in SCM layer (Fujiki and Taguchi, 2002; Fu et al., 2018). With the abrupt enhancement of light intensity (from SCM to surface), phytoplankton in the incubated seawater need to readjust to the new environment and thus showed a limited response to AR additions.

Interestingly, AR addition had a significant fertilization effect on phytoplankton growth at U1$_{SCM}$ (**Figure 4**), which was characterized by the higher trophic status among these sites. Note that there was a shift in dominant phytoplankton from picosized cells to large cells during the incubations at U1$_{SCM}$, which was different from the sustaining dominance of picosized cells at U3$_{SCM}$ (**Figure 5**). Moreover, large phytoplankton can better acclimate to the abrupt increase in light intensity compared with picosized cells, due to their stronger self-shading capacity by the pigment (package effect) to reduce light absorption (Marañón, 2015). At U2$_{SCM}$, the stimulation effect of AR addition was not

as obvious as that at U1$_{SCM}$ (**Figure 4**). This is because there was an obvious shift of dominant algae from Coscinodiscophyceae in the control to Dinophyceae in the AR treatments at U2$_{SCM}$ (**Figure 6**). The obvious succession in phytoplankton community while slight change in Chl *a* under the condition of aerosol enrichment was also observed in eutrophic seawaters of the ECS (Meng et al., 2016). The substantial input of N relative to P supplied by AR addition increased the N:P ratio from 24:1 in the original seawater to 28:1 in the AR treatments at U2$_{SCM}$, which was more favorable for the growth of dinoflagellates (Zhang et al., 2019; **Table 2**). At U1$_{SCM}$, in contrast, the N:P ratio ranged between 10:1 and 16:1 in the control and AR treatments, leading to the increase in relative abundance of diatoms (primarily Coscinodiscophyceae) (Zhang et al., 2019). Collectively, in contrast to the consistent phytoplankton response to AR addition in surface seawater, the impact of AR addition in SCM seawater is complicated, which is closely related to nutrient concentration and structure in seawater.

Utilization of Dissolved Organic P Enhanced by Anthropogenic Aerosol Addition

The substantial N supplied by AR had the potential to alleviate and even alter N pressure of phytoplankton in the incubated

FIGURE 7 | Correlations between species (level 3) and environmental factors based on redundancy analysis (RDA).

FIGURE 8 | The relationship between APA and the contribution of microsized Chl a to the total Chl a in the AR treatments **(A)** and the relationship between relative change in APA (RC_{APA}) and nanosized+picosized Chl a ($RC_{Nano+Pico}$) in the unfiltered seawater relative to the filtered seawater **(B)**. RC_{APA} and $RC_{Nano+Pico}$ was calculated as ([mean in the unfiltered seawater - mean in the filtered seawater]/mean in the filtered seawater) × 100. The contribution of microsized Chl a to the total Chl a in the control was less than 15% throughout the experiments, and thus, there was no incubations with filtered seawater at $U2_{Sur}$.

seawater (**Figure 2**). As a result, the relatively P-deficient environment created by AR additions made it possible for phytoplankton to induce acclimatization mechanisms to copy with P stress (Moore et al., 2013). As shown in **Figure 3**, the APA value in the AR treatments was higher than that of the control at the end of the incubations at all sites, indicating that AR

could enhance the utilization of DOP to increase P bioavailability in the incubated seawater. Such phenomenon was supported by the good correlation between PO_4^{3-} and APA (**Figure 7**). In apart from the establishment of P-deficient environment, AR additions also provided a considerable amount of soluble Fe and Zn, which acted as cofactors of phosphohydrolytic

enzymes (Mills et al., 2004; Mahaffey et al., 2014). The promotion effect of AR addition on the utilization of DOP shows the acclimation of phytoplankton to the overwhelming N input relative to P in coastal waters (Zhang et al., 1999; Zamora et al., 2010; Xing et al., 2017) and is conductive to understanding P biogeochemical cycles in the perspective of atmospheric deposition.

In terms of the phytoplankton community composition, Dinophyceae generally dominated the community in UFS enriched with AR at all sites (**Figure 6**). With relatively high tolerance to nutrient-deficient environments and the potential to utilize DOP by inducing the expression of the gene for the synthesis of AP (Lin et al., 2012), dinoflagellates showed an advantageous growth in the AR treatments. This is also the reason why nutrient limitation had a slight impact on the growth of Dinophyceae based on RDA (**Figure 7**). In addition, due to the selective feeding of micrograzers, picosized phytoplankton suffer from a higher grazing pressure (Cottingham, 1999; Strom et al., 2007). In contrast, large dinoflagellates have the ability to keep themselves away from the prey of the dominant zooplankton species *Paracalanus parvus* (Hexanauplia) through particle rejection behavior (reject particles as food, **Supplementary Figure 4**; Huntley et al., 1986; Tiselius et al., 2013).

Role of Microsized Phytoplankton in Affecting the Growth of Nanosized and Picosized Phytoplankton

As described in "Changes in Total and Size-Fractionated chlorophyll *a*" section at $U1_{Sur}$, $U3_{Sur}$, and $U3_{SCM}$ characterized by lower trophic statuses, the nanosized and picosized Chl *a* concentrations in FS enriched with AR were lower than those in UFS. In contrast, we did not observe similar results at $U1_{SCM}$ and $U2_{SCM}$ characterized by higher trophic statuses (**Figure 4**).

Nutrients, irradiance, and temperature are considered the three major factors that affect phytoplankton growth (Laws et al., 2000; Litchman, 2007). There was no difference in light and temperature between UFS and FS, and thus, nutrients play a key role in causing the lower nanosized and picosized Chl *a* concentrations in FS. At $U1-3_{Sur}$ and $U3_{SCM}$, there were no obvious differences in N + N and PO_4^{3-} between UFS and FS (**Figure 2**). Meanwhile, we found that the APA values in UFS were 1.6-7.3 times higher than those in FS (**Figure 3**), indicating that microsized cells played an important role in increasing P bioavailability in the incubated seawater (Sebastián et al., 2004). This was supported by the positive linear relationship between APA and the contribution of microsized cells to the total Chl *a* (**Figure 8A**). As an extracellular enzyme, AP enters the environment through autolyzing or organisms excreting (Štrojsová et al., 2003). Besides, in contrast to FS, nanosized and picosized Chl *a* concentration in UFS increased linearly with relative change of APA (**Figure 8B**). Therefore, under the impact of AR addition, microsized cells have the ability

to favor the growth of nanosized and picosized cells by increasing P bioavailability in seawater. The result at $U1_{SCM}$ characterized by higher trophic statuses could also support this argument. On days 1-2 of the incubations, there was no difference in the nanosized and picosized Chl *a* concentrations in the AR treatments between UFS and FS when PO_4^{3-} was sufficient in the seawater, but lower nanosized and picosized Chl *a* concentrations in FS were measured when PO_4^{3-} was exhausted on day 3 (**Figures 2**, **4**). Besides, dinoflagellates and green algae with the capacity of utilizing DOP also showed advantageous growth in the P-deficient condition (**Figure 6**).

There are other factors that might have caused the mismatch between UFS and FS in the concentration of nanosized and picosized Chl *a*. For example, the biodiversity of the community decreased after removal of microsized cells, which increased the difficulty for the community to reestablish a new balance (Dyke et al., 2007). Nanosized and picosized phytoplankton may adopt a strategy to survive in unstable habitats, e.g., by producing spores that can be dormant temporarily and revive at an appropriate time (Nayaka et al., 2017). However, these inferences cannot account for the change in nanosized and picosized Chl *a* at $U1_{SCM}$ and $U2_{SCM}$ characterized by higher trophic statuses (**Figure 4**). Therefore, our study provides a new clue from the perspective of nutrient utilization to illustrate how microsized phytoplankton affect the growth of nanosized and picosized ones.

CONCLUSION

In this study, we conducted three onboard incubation experiments using surface and SCM seawaters under the condition of sea surface light intensity in the Yellow Sea and East China Sea. AR addition generally stimulated phytoplankton growth in surface incubations and had a stimulatory or slight impact in SCM incubations, which primarily depends on the nutrient concentration and structure in seawater. We also found that AR addition could alleviate P limitation by promoting the utilization of DOP in both surface and SCM incubations. Specifically in seawater with lower trophic status, microsized cells have the ability to promote the growth of nanosized and picosized cells by increasing P bioavailability in the incubated seawater. Considering the lower contribution of microsized cells in the oligotrophic areas of the open oceans (López-Urrutia and Morán, 2015; Marañón et al., 2015), such a promotion effect of microsized cells induced by anthropogenic aerosol deposition may focus on coastal waters and thus can be regarded as a result of anthropogenic influences to a large extent. With the enhanced influence of human activities in the recent years, atmospheric deposition characterized by high N:P ratios has intensified the prevailing P limitation in offshore waters (Harrison et al., 1990; Xu et al., 2008). The acclimation mechanism of different sized phytoplankton to P limitation under the influence of atmospheric deposition deserves to be further investigated.

DATA AVAILABILITY STATEMENT

The datasets presented in this study can be found in online repositories. The names of the repository/repositories and accession number(s) can be found in the article/**Supplementary Material**.

AUTHOR CONTRIBUTIONS

QW: conceptualization, investigation, methodology, data curation, formal analysis, visualization, software, and writing – original draft. CZ: conceptualization, investigation, writing – review and editing, data curation, and funding acquisition. HJ: investigation. YC and XY: writing – review and editing. HG: supervision, methodology, resources, writing – review and editing, and funding acquisition and also was responsible for ensuring that the descriptions are accurate and agreed by all authors. All authors contributed to the article and approved the submitted version.

FUNDING

SUPPLEMENTARY MATERIAL

The Supplementary Material for this article can be found online at: https://www.frontiersin.org/articles/10.3389/fmicb.2022.915255/full#supplementary-material

REFERENCES

Agusti, S., and Kalff, J. (1989). The influence of growth conditions on the size dependence of maximal algal density and biomass. *Limnol. Oceanogr.* 34, 1104–1108. doi: 10.4319/lo.1989.34.6.1104

An, Z., Huang, R., Zhang, R., Tie, X., Li, G., and Cao, J. (2019). Severe haze in northern China: a synergy of anthropogenic emissions and atmospheric processes. *Proc. Natl. Acad. Sci. U.S.A.* 116, 8657–8666. doi: 10.1073/pnas.1900125116

Andersen, I. M., Williamson, T. J., González, M. J., and Vanni, M. J. (2020). Nitrate, ammonium, and phosphorus drive seasonal nutrient limitation of chlorophytes, cyanobacteria, and diatoms in a hyper-eutrophic reservoir. *Limnol. Oceanogr.* 65, 962–978. doi: 10.1002/lno.11363

Bokulich, N. A., Kaehler, B. D., Rideout, J. R., Dillon, M., Bolyen, E., and Knight, R. (2018). Optimizing taxonomic classification of marker-gene amplicon sequences with QIIME 2's q2-feature-classifier plugin. *Microbiome* 6:90. doi: 10.1186/s40168-018-0470-z

Boyd, P. W., Jickells, T., Law, C. S., Blain, S., Boyle, E. A., and Buesseler, K. O. (2007). Mesoscale iron enrichment experiments 1993-2005: synthesis and future directions. *Science* 315, 612–617. doi: 10.1126/science.1131669

Browning, T. J., Achterberg, E. P., Yong, J. C., Rapp, I., Utermann, C., and Engel, A. (2017). Iron limitation of microbial phosphorus acquisition in the tropical North Atlantic. *Nat. Commun.* 8:15465. doi: 10.1038/ncomms15465

Callahan, B. J., Mcmurdie, P. J., Rosen, M. J., Han, A. W., Johnson, A. J. A., and Holmes, S. P. (2016). DADA2: high-resolution sample inference from Illumina amplicon data. *Nat. Methods* 13, 581–583. doi: 10.1038/nmeth.3869

Chisholm, S. W. (1992). "Phytoplankton Size," in *Primary Productivity and Biogeochemical Cycles in the Sea*, eds P. G. Falkowski, A. D. Woodhead, and K. Vivirito (Boston, MA: Springer), 213–237.

Chu, Q., Liu, Y., Shi, J., Zhang, C., Gong, X., and Yao, X. (2018). Promotion effect of Asian dust on phytoplankton growth and potential dissolved organic phosphorus utilization in the South China Sea. *J. Geophys. Res. Biogeosci.* 123, 1101–1116. doi: 10.1002/2017JG004088

Cottingham, K. L. (1999). Nutrients and zooplankton as multiple stressors of phytoplankton communities: evidence from size structure. *Limnol. Oceanogr.* 44, 810–827.

Du, J., Cheng, T., Zhang, M., Chen, J., He, Q., and Wang, X. (2012). Aerosol size spectra and particle formation events at urban Shanghai in Eastern China. *Aerosol Air Qual. Res.* 12, 1362–1372. doi: 10.4209/aaqr.2011.12.0230

Dyke, J., Mcdonald-Gibson, J., Di Paolo, E., Harvey, I. (2007). "Increasing Complexity Can Increase Stability in a Self-Regulating Ecosystem," in *Advances in Artificial Life. ECAL 2007. Lecture Notes in Computer Science*, eds E Almeida F Costa., L.M Rocha., E Costa., I Harvey., and A Coutinho (Berlin: Springer), 133-142.

Finkel, Z. V. (2007). "Chapter 15 - Does phytoplankton cell size matter? The Evolution of Modern Marine Food Webs," in *Evolution of Primary Producers in the Sea*, eds P. G. Falkowski and A. H. Knoll (Burlington: Academic Press), 333–350.

Fu, H., Zheng, M., Yan, C., Li, X., Gao, H., and Yao, X. (2015). Sources and characteristics of fine particles over the Yellow Sea and Bohai Sea using online single particle aerosol mass spectrometer. *J. Environ. Sci. China* 29, 62–70. doi: 10.1016/j.jes.2014.09.031

Fu, M., Sun, P., Wang, Z., Wei, Q., Qu, P., and Zhang, X. (2018). Structure, characteristics and possible formation mechanisms of the subsurface chlorophyll maximum in the Yellow Sea Cold Water Mass. *Cont. Shelf Res.* 165, 93–105. doi: 10.1016/j.csr.2018.07.007

Fujiki, T., and Taguchi, S. (2002). Variability in chlorophyll a specific absorption coefficient in marine phytoplankton as a function of cell size and irradiance. *J. Plankton Res.* 24, 859–874. doi: 10.1093/plankt/24.9.859

Gong, X., Jiang, W., Wang, L., Gao, H., Boss, E., and Yao, X. (2017). Analytical solution of the nitracline with the evolution of subsurface chlorophyll maximum in stratified water columns. *J. Geophys. Res. Biogeosci.* 14, 2371–2386. doi: 10.5194/bg-14-2371-2017

Granéli, E., Carlsson, P., and Legrand, C. (1999). The role of C, N and P in dissolved and particulate organic matter as a nutrient source for phytoplankton growth, including toxic species. *Aquat. Ecol.* 33, 17–27. doi: 10.1023/A:1009925515059

Guo, C., Jing, H., Kong, L., and Liu, H. (2013). Effect of East Asian aerosol enrichment on microbial community composition in the South China Sea. *J. Plankton Res.* 35, 485–503. doi: 10.1093/plankt/fbt002

Harrison, P. J., Hu, M. H., Yang, Y. P., and Lu, X. (1990). Phosphate limitation in estuarine and coastal waters of China. *J. Exp. Mar. Biol. Ecol.* 140, 79–87. doi: 10.1016/0022-0981(90)90083-O

Heisler, J., Glibert, P. M., Burkholder, J. M., Anderson, D. M., Cochlan, W., and Dennison, W. C. (2008). Eutrophication and harmful algal blooms: a scientific consensus. *Harmful Algae* 8, 3–13. doi: 10.1016/j.hal.2008.08.006

Hernández-Ruiz, M., Barber-Lluch, E., Prieto, A., Logares, R., and Teira, E. (2020). Response of pico-nano-eukaryotes to inorganic and organic nutrient additions. *Estuar. Coast. Shelf Sci.* 235:106565. doi: 10.1016/j.ecss.2019.106565

Hodges, B. A., and Rudnick, D. L. (2004). Simple models of steady deep maxima in chlorophyll and biomass. *Deep Sea Res. Part I Oceanogr. Res. Pap.* 51, 999–1015. doi: 10.1016/j.dsr.2004.02.009

Hooper, J., Mayewski, P., Marx, S., Henson, S., Potocki, M., and Sneed, S. (2019). Examining links between dust deposition and phytoplankton response using ice cores. *Aeolian Res.* 36, 45–60. doi: 10.1016/j.aeolia.2018.11.001

Huntley, M., Sykes, P., Rohan, S., and Marin, V. (1986). Chemically-mediated rejection of dinoflagellate prey by the copepods *Calanus pacificus* and *Paracalanus parvus*: mechanism, occurrence and significance. *Mar. Ecol. Prog. Ser.* 28, 105–120. doi: 10.3354/meps028105

Hutchins, D. A., Witter, A. E., Butler, A., and Luther, G. W. (1999). Competition among marine phytoplankton for different chelated iron species. *Nature* 400, 858–861. doi: 10.1038/23680

Jickells, T. D., An, Z. S., Andersen, K. K., Baker, A. R., Bergametti, G., Brooks, N., et al. (2005). Global iron connections between desert dust, ocean biogeochemistry, and climate. *Science* 5718, 67–71. doi: 10.1126/science.1105959

Kang, M., Yang, F., Ren, H., Zhao, W., Zhao, Y., and Li, L. (2017). Influence of continental organic aerosols to the marine atmosphere over the East China Sea: insights from lipids, PAHs and phthalates. *Sci. Total Environ.* 60, 339–350. doi: 10.1016/j.scitotenv.2017.06.214

Kim, T., Lee, K., Duce, R., and Liss, P. (2014). Impact of atmospheric nitrogen deposition on phytoplankton productivity in the South China Sea. *Geophys. Res. Lett.* 41, 3156–3162. doi: 10.1002/2014GL059665

Krishnamurthy, A., Moore, J. K., Zender, C. S., and Luo, C. (2007). Effects of atmospheric inorganic nitrogen deposition on ocean biogeochemistry. *J. Geophys. Res. Biogeosci.* 112:G02019. doi: 10.1029/2006JG000334

Laws, E. A., Falkowski, P. G., Smith, W. O. Jr., Ducklow, H., and Mccarthy, J. J. (2000). Temperature effects on export production in the open ocean. *Global Biogeochem. Cy.* 14, 1231–1246. doi: 10.1029/1999GB001229

Lin, X., Zhang, H., Cui, Y., and Lin, S. (2012). High sequence variability, diverse subcellular localizations, and ecological implications of alkaline phosphatase in Dinoflagellates and other eukaryotic phytoplankton. *Front. Microbiol.* 3:235. doi: 10.3389/fmicb.2012.00235

Litchman, E. (2007). "Chapter 16 - Resource competition and the ecological success of phytoplankton," in *Evolution of Primary Producers in the Sea*, eds P. G. Falkowski and A. H. Knoll (Burlington: Academic Press), 351–375.

Liu, Q., Zhao, Q., McMinn, A., Yang, E. J., and Jiang, Y. (2021). Planktonic microbial eukaryotes in polar surface waters: recent advances in high-throughput sequencing. *J. Mar. Sci. Technol.* 3, 94–102. doi: 10.1007/s42995-020-00062-y

Liu, Y., Zhang, T. R., Shi, J. H., Gao, H. W., and Yao, X. H. (2013). Responses of chlorophyll a to added nutrients, Asian dust, and rainwater in an oligotrophic zone of the Yellow Sea: implications for promotion and inhibition effects in an incubation experiment. *J. Geophys. Res. Biogeosci.* 118, 1763–1772. doi: 10.1002/2013JG002329

López-Urrutia, Á, and Morán, X. A. G. (2015). Temperature affects the size-structure of phytoplankton communities in the ocean. *Limnol. Oceanogr.* 60, 733–738. doi: 10.1002/lno.10049

Mahaffey, C., Reynolds, S., Davis, C. E., and Lohan, M. C. (2014). Alkaline phosphatase activity in the subtropical ocean: insights from nutrient, dust and trace metal addition experiments. *Front. Mar. Sci.* 1:73. doi: 10.3389/fmars.2014.00073

Marañón, E. (2015). Cell size as a key determinant of phytoplankton metabolism and community structure. *Ann. Rev. Mar. Sci.* 7, 241–264. doi: 10.1146/annurev-marine-010814-015955

Marañón, E., Cermeño, P., Latasa, M., and Tadonléké, R. D. (2015). Resource supply alone explains the variability of marine phytoplankton size structure. *Limnol. Oceanogr.* 60, 1848–1854. doi: 10.1002/lno.10138

Martin, M. (2011). Impacts of atmospheric deposition on phytoplankton community structure in the Yellow Sea. *EMBnet. J.* 17, 10–12. doi: 10.14806/ej.17.1.200

Meng, X., Chen, Y., Wang, B., Ma, Q. W., and Wang, F. J. (2016). Responses of phytoplankton community to the input of different aerosols in the East China Sea. *Geophys. Res. Lett.* 43, 7081–7088. doi: 10.1002/2016GL069068

Mills, M. M., Ridame, C., Davey, M., La Roche, J., and Geider, R. J. (2004). Iron and phosphorus co-limit nitrogen fixation in the eastern tropical North Atlantic. *Nature* 429, 292–294. doi: 10.1038/nature02550

Moore, C. M., Mills, M. M., Arrigo, K. R., Berman-Frank, I., Bopp, L., Boyd, P. W., et al. (2013). Processes and patterns of oceanic nutrient limitation. *Nat. Geosci.* 6, 701–710. doi: 10.1038/ngeo1765

Nayaka, S., Toppo, K., and Verma, S. (2017). "Adaptation in algae to environmental stress and ecological conditions," in *Plant Adaptation Strategies in Changing Environment*, eds V. Shukla, S. Kumar, and N. Kumar (Berlin: Springer), 103–115.

Okin, G. S., Baker, A. R., Tegen, I., Mahowald, N. M., Dentener, F. J., and Duce, R. A. (2011). Impacts of atmospheric nutrient deposition on marine productivity: roles of nitrogen, phosphorus, and iron. *Glob. Biogeochem. Cy.* 25:GB2022. doi: 10.1029/2010GB003858

Pasciak, W. J., and Gavis, J. (1974). Transport limitation of nutrient uptake in phytoplankton1. *Limnol. Oceanogr.* 19, 881–888. doi: 10.4319/lo.1974.19.6.0881

Quast, C., Pruesse, E., Yilmaz, P., Gerken, J., Schweer, T., and Yarza, P. (2013). The SILVA ribosomal RNA gene database project: improved data processing and web-based tools. *Nucleic Acids Res.* 41, D590–D596. doi: 10.1093/nar/gks1219

Sebastián, M., Arístegui, J., Montero, M. F., Escanez, J., and Xavier Niell, F. (2004). Alkaline phosphatase activity and its relationship to inorganic phosphorus in the transition zone of the North-western African upwelling system. *Prog. Oceanogr.* 62, 131–150. doi: 10.1016/j.pocean.2004.07.007

Shi, J., Gao, H., Qi, J., Zhang, J., and Yao, X. (2010). Sources, compositions, and distributions of water-soluble organic nitrogen in aerosols over the China Sea. *J. Geophys. Res. Atmos.* 115:D17303. doi: 10.1029/2009JD013238

Shi, J., Gao, H., Zhang, J., Tan, S., Ren, J., and Liu, C. (2012). Examination of causative link between a spring bloom and dry/wet deposition of Asian dust in the Yellow Sea, China. *J. Geophys. Res. Atmos.* 117:2012. doi: 10.1029/2012JD017983

Sin, Y., Hyun, B., Jeong, B., and Soh, H. Y. (2013). Impacts of eutrophic freshwater inputs on water quality and phytoplankton size structure in a temperate estuary altered by a sea dike. *Mar. Environ. Res.* 85, 54–63. doi: 10.1016/j.marenvres.2013.01.001

Stolte, W., and Riegman, R. (1996). A model approach for size-selective competition of marine phytoplankton for fluctuating nitrate and ammonium1. *J. Phycol.* 32, 732–740. doi: 10.1111/j.0022-3646.1996.00732.x

Štrojsová, A., Vrba, J., Nedoma, J., Komárková, J., and Znachor, P. (2003). Seasonal study of extracellular phosphatase expression in the phytoplankton of a eutrophic reservoir. *Eur. J. Phycol.* 38, 295–306. doi: 10.1080/0967026031000161628

Strom, S. L., Macri, E. L., and Olson, M. B. (2007). Microzooplankton grazing in the coastal gulf of Alaska: variations in top-down control of phytoplankton. *Limnol. Oceanogr.* 52, 1480–1494. doi: 10.4319/lo.2007.52.4.1480

Tan, S., and Shi, G. (2012). Transport of a severe dust storm in March 2007 and impacts on chlorophyll a concentration in the Yellow Sea. *SOLA* 8, 85–89. doi: 10.2151/sola.2012-022

Tan, S., and Wang, H. (2014). The transport and deposition of dust and its impact on phytoplankton growth in the Yellow Sea. *Atmos. Environ.* 99, 491–499. doi: 10.1016/j.atmosenv.2014.10.016

Tiselius, P., Saiz, E., and Kiørboe, T. (2013). Sensory capabilities and food capture of two small copepods, Paracalanus parvus and Pseudocalanus sp. *Limnol. Oceanogr.* 58, 1657–1666. doi: 10.4319/lo.2013.58.5.1657

Wang, D., Huang, B., Liu, X., Liu, G., and Wang, H. (2014). Seasonal variations of phytoplankton phosphorus stress in the Yellow Sea Cold Water Mass. *Acta Oceanol. Sin.* 33, 124–135. doi: 10.1007/s13131-014-0547-x

Wang, S., Arthur Chen, C., Hong, G., and Chung, C. (2000). Carbon dioxide and related parameters in the East China Sea. *Cont. Shelf Res.* 20, 525–544. doi: 10.1016/S0278-4343(99)00084-9

Wei, Y., Sun, J., Zhang, X., Wang, J., and Huang, K. (2019). Picophytoplankton size and biomass around equatorial eastern Indian Ocean. *MicrobiologyOpen* 8:e00629. doi: 10.1002/mbo3.629

Wu, Y., Zhang, J., Liu, S., Jiang, Z., and Huang, X. (2018). Aerosol concentrations and atmospheric dry deposition fluxes of nutrients over Daya Bay, South China Sea. *Mar. Pollut. Bull.* 128, 106–114. doi: 10.1016/j.marpolbul.2018.01.019

Xiao, H. W., Xiao, H. Y., Shen, C. Y., Zhang, Z. Y., and Long, A. M. (2018). Chemical composition and sources of marine aerosol over the Western North Pacific Ocean in winter. *Atmosphere* 9:298. doi: 10.3390/atmos9080298

Xing, J., Song, J., Yuan, H., Li, X., Li, N., Duan, L., et al. (2017). Fluxes, seasonal patterns and sources of various nutrient species (nitrogen, phosphorus and silicon) in atmospheric wet deposition and their ecological effects on Jiaozhou Bay, North China. *Sci. Total Environ.* 576, 617–627. doi: 10.1016/j.scitotenv.2016.10.134

Xu, J., Yin, K., He, L., Yuan, X., Ho, A. Y. T., and Harrison, P. J. (2008). Phosphorus limitation in the northern South China Sea during late summer: influence of

the Pearl River. *Deep Sea Res. Part I Oceanogr.* 55, 1330–1342. doi: 10.1016/j.dsr.2008.05.007

Zamora, L. M., Landolfi, A., Oschlies, A., Hansell, D. A., Dietze, H., and Dentener, F. (2010). Atmospheric deposition of nutrients and excess N formation in the North Atlantic. *J. Geophys. Res. Biogeosci.* 7, 777–793. doi: 10.5194/bg-7-777-2010

Zhang, C., Gao, H., Yao, X., Shi, Z., Shi, J., and Yu, Y. (2018). Phytoplankton growth response to Asian dust addition in the northwest Pacific Ocean versus the Yellow Sea. *J. Geophys. Res. Biogeosci.* 15, 749–765. doi: 10.5194/bg-15-749-2018

Zhang, C., He, J., Yao, X., Mu, Y., Guo, X., and Ding, X. (2020). Dynamics of phytoplankton and nutrient uptake following dust additions in the northwest Pacific. *Sci. Total Environ.* 739:139999. doi: 10.1016/j.scitotenv.2020.139999

Zhang, C., Yao, X., Chen, Y., Chu, Q., Yu, Y., and Shi, J. (2019). Variations in the phytoplankton community due to dust additions in eutrophication, LNLC and HNLC oceanic zones. *Sci. Total Environ.* 669, 282–293. doi: 10.1016/j.scitotenv.2019.02.068

Zhang, J., Chen, S. Z., Yu, Z. G., Wang, C. S., and Wu, Q. M. (1999). Factors influencing changes in rainwater composition from urban versus remote regions of the Yellow Sea. *J. Geophys. Res. Atmos.* 104, 1631–1644. doi: 10.1029/1998JD100019

Zhang, K., and Gao, H. (2007). The characteristics of Asian-dust storms during 2000-2002: from the source to the sea. *Atmos. Environ.* 41, 9136–9145. doi: 10.1016/j.atmosenv.2007.08.007

Zhao, R., Han, B., Lu, B., Zhang, N., Zhu, L., and Bai, Z. (2015). Element composition and source apportionment of atmospheric aerosols over the China Sea. *Atmos. Pollut. Res.* 6, 191–201. doi: 10.5094/APR.2015.023

Zheng, L., and Zhai, W. (2021). Excess nitrogen in the Bohai and Yellow seas, China: distribution, trends, and source apportionment. *Sci. Total Environ.* 794:148702. doi: 10.1016/j.scitotenv.2021.148702